

Krzysztof Ostrowski (kostrow@agh.edu.pl)

Konrad Oleksik (koleksik@agh.edu.pl)

Faculty of Mining and Geoengineering, AGH University of Science and Technology

## COMPARATIVE ANALYSIS OF THE COARSE AGGREGATE SHAPES USED TO MANUFACTURING HIGH PERFORMANCE SELF-COMPACTING CONCRETE

### ANALIZA PORÓWNAWCZA KSZTAŁTU KRUSZYW STOSOWANYCH W PRODUKCJI WYSOKOWARTOŚCIOWYCH BETONÓW SAMOZAGĘSZCZALNYCH

#### Abstract

The influence of the shape of coarse aggregate on the properties of fresh concrete mixes, and the strength of high-performance self-compacting concrete (HPSCC) is important issue. In this study, irregular and regular grains were separated from the basalt, porphyry and granite coarse aggregate. The shape of these grains was determined using digital image analysis and was in accordance with the European Standard [19]. The aspect ratio (AR) and roundness (R) were ascertained in order to highlight the differences in the coarse aggregate shape used in the design HPSCC. The study indicates that using the same crushing system, varied parameters of the shape of coarse aggregates were obtained. It was determined that the best fitting distribution for aspect ratio and roundness at a 95% confidence level is the generalised extreme value distribution.

**Keywords:** coarse aggregate, shape, computer image analysis, self-compacting concrete

#### Streszczenie

Wpływ kształtu kruszywa grubego na właściwości świeżej mieszanki betonowej i wytrzymałość samozagęszczalnego betonu wysokowartościowego (HPSCC) są bardzo znaczące. W badaniach wydzielono nieregularne i regularne ziarna kruszyw, takich jak bazalt, porfir i granit. Kształt ziaren tych kruszyw został wyznaczony przy pomocy komputerowej analizy obrazu oraz w zgodzie z obowiązującą normą. W rezultacie zostały wyznaczone wskaźniki kształtu kruszywa, takie jak AR i R, w celu podkreślenia różnic w kształcie kruszyw stosowanych do produkcji betonów HPSCC. Badania wskazują, iż przy zastosowaniu tego samego systemu kruszenia uzyskano różne parametry kształtu dla analizowanych kruszyw. Stwierdzono, iż wskaźniki kształtu kruszywa AR oraz R mogą być opisywane poprzez rozkład uogólnionej wartości ekstremalnej na poziomie istotności wynoszącym 95%.

**Słowa kluczowe:** kruszywo, kształt, komputerowa analiza obrazu, beton samozagęszczalny.

## 1. Introduction

Self-compacting concrete (SCC) was developed in 1988 [15] and since then, it has been widely used in the construction industry due to the fact that the laying and quality control of SCC are easier than those of conventional vibrated concrete (CVC); this is because of its characteristics of super fluidity and self-consolidation [23]. Use of SCC has brought substantial advantages to the productivity of construction work [4]. Currently, SCC is used in many developing countries for versatile applications, such as high-rise skyscrapers, urban infrastructure and structural configurations [6]. By using appropriate constituent materials such as Portland cement, the new generation of superplasticizer silica fume, and coarse aggregate, it is possible to obtain HPSCC.

Coarse aggregate is a very important proportion of the concrete volume and therefore has a major influence on its quality [11]. This is especially true in the case of HPSCC, where the quality of coarse aggregate determines the behaviour of the concrete. In Poland, the following main aggregates are used for the production of HPSCC: basalt, granite, diabase, porphyry [9]. This material is characterised by its high bulk density, mechanical strength and Young's modulus.

In the concrete industry, HPSCC mixes mostly use aggregates comprised of magmatic rocks. The type of rocks, their mineralogical composition and crushing manner are the main elements which influence the shape of coarse aggregate. It has been widely shown that the type of crusher plays an important role in the manufacturing of the aggregates and in their different shape parameters [20].

Considering the importance of the shape of aggregate components, the aim of this study is to present a comparative analysis of the coarse aggregate shapes used to produce HPSCC using the examples of granite, basalt and porphyry. The rest of the paper is organised as follows: Section 2 presents the research significance; Section 3 presents the literature; Section 4 presents materials and methods; Section 5 presents the test results and discussion; Section 6 presents the conclusions.

## 2. Research significance

In general, during design of HPSCC mixes we take into account the quantity and type of binder, the type of admixtures affecting the rheology of the concrete mixture and the granular class of the aggregate. As is widely known, SCC is characterised by properties such as: flowability, segregation resistance and passing ability. It transpires that the shape of the aggregate grains affects these parameters which define SCC. The condition for gain HPSCC is also the use of broken aggregates of high strength mainly obtained from igneous rocks. Therefore, the authors decided to analyse how the shape parameters of different aggregates used in the production of HPSCC are changed during the crushing process. In this study, coarse aggregates of basalt, granite and porphyry were analysed.

### 3. Literature survey

It has been showed many times that coarse aggregates of the same type and composition but with random angularity indices and aspect ratios have an impact on the mechanical properties of the concrete [22]. The interaction between specific surfaces of the coarse aggregate and the difference in densities between the aggregate and the mortar phase can be considered to be the explanation for this phenomenon [21]. The segregation of concrete mixture which ultimately influences the strength and durability of concrete, is one of the major problems that occurs during construction. The segregation tendency of concrete mixture is primarily apparent in the difference in density between the aggregate and the mortar phase [14]. This is crucial aspect in design HPSCC, where bulk density of coarse aggregate could be more than  $3000 \text{ kg/m}^3$  in the case of basalt.

It has already been proven that the cement paste content and water/binder ratio are significant parameters of the mix design due to the appropriate rheological properties [8]. Ostrowski et al. [18] showed that the shape of the grain aggregate has a significant impact on the rheological parameters of concrete mixture. It has been revealed that usage of regular grains of coarse aggregate causes a higher slump flow and a lower plastic viscosity of concrete mixtures in comparison to situations in which the aggregate is comprised of irregular grains. Experimental research [16] has indicated that the difference in the slump flow of concrete mixtures in the case of using regular and irregular coarse aggregate can reach 150 mm. Furthermore, the type of the coarse aggregate shape determines the compressive strength of concrete. The importance of coarse aggregate in designing and predicting the behaviour of SCC has been emphasised many times [7]. In comparison to normal concrete, the mix design of HPSCC is more difficult and should take into account adequate static and dynamic stability. The selection of coarse aggregate is a significant parameter for the mix design and mixture optimisation of HPSCC.

There are many indicators to assess the shape of the particles; these can be divided into two groups. The first group is made up of two-dimensional shape factors such as aspect ratio [10], roundness, sphericity [1] and area ratio [2]. The second group is comprised of three-dimensional shape factors such as flat and elongation ratios [1].

### 4. Materials and methods

The feed material was basalt and porphyry with a maximum size of 200 mm. The material was separately crushed and sieved in a laboratory-scale comminution circuit (Fig. 1).

The final product (4–8 mm) from comminution was then sieved into three grades: 4–5 mm, 5–6.3 mm and 6.3–8 mm with the use of square sieves. In the next step, each narrow grade was sieved with the use of bar sieves, in line with the European Standard [19]. The bar sieves (Fig. 2) were selected to be about half of the maximum size of certain fraction's particles ( $d_{\text{max}}/2$ ):

- ▶ 2.5 mm for 4–5 mm grade fraction
- ▶ 3.15 mm for 5–6.3 mm grade fraction
- ▶ 4 mm for 6.3–8 mm grade fraction

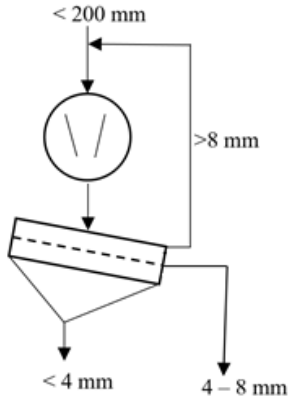


Fig. 1. Comminution circuit with jaw crusher



Fig. 2. Laboratory bar sieves.

On the basis of the sieve analysis, the particle-size distribution for each of the examined materials was plotted (Figs. 3a, 3b). Particle-size distributions of granite were based on the article in [17] (Fig. 4).

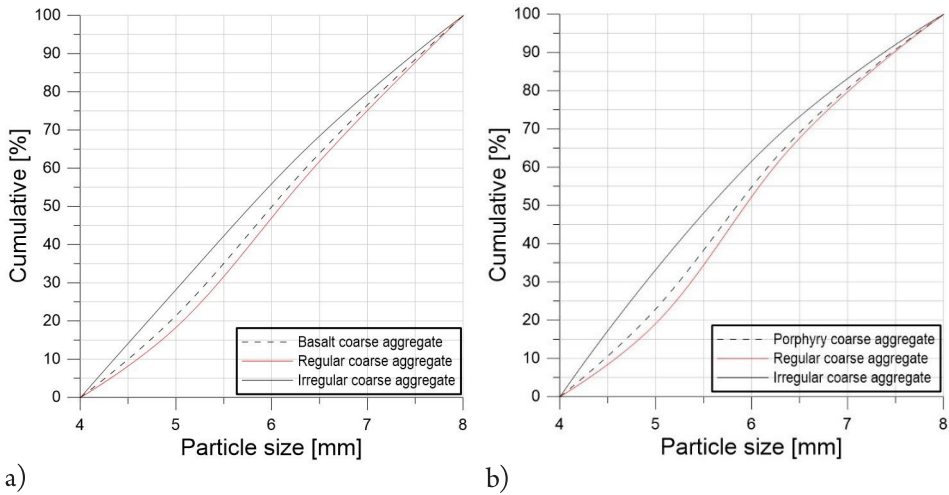


Fig. 3. Particle-size distribution of: a) prepared basalt coarse aggregate; b) porphyry coarse aggregate

For each type of coarse aggregate, Flakiness Index (FI) was performed [19].

$$FI = \frac{M_2}{M_1} \cdot 100 \quad (1)$$

where:

$M_2$  – mass of irregular grains

$M_1$  – mass of regular and irregular grains

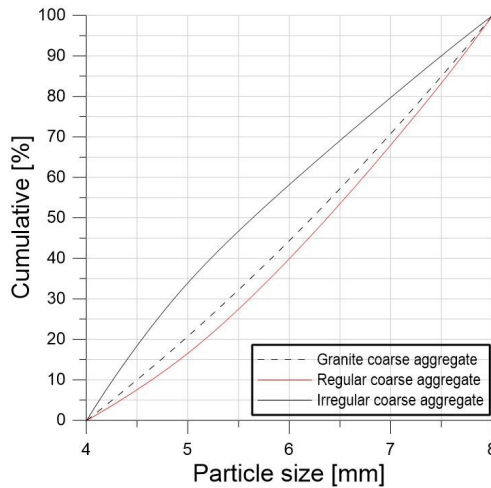


Fig. 4. Particle-size distribution of prepared granite coarse aggregate [17]

The FI for basalt, porphyry and granite was 32%, 27% and 24%, respectively. The same crushing process yielded the highest content of regular grains for granite and the lowest content of regular grains for basalt. Circuits with closed recirculation for selective screening and crushing operations designed by Gawenda [3] allows the obtaining of final aggregates with contents of less than 2–3% of irregular particles.

Representative samples of coarse aggregate were selected for computer image analysis while maintaining the percentage mass fraction of particular particle-size grades:

- ▶ 0.05 kg of regular basalt coarse aggregate
- ▶ 0.05 kg of irregular basalt coarse aggregate
- ▶ 0.05 kg of regular porphyry coarse aggregate
- ▶ 0.05 kg of irregular porphyry coarse aggregate

High resolution photos were taken of the samples' with adequate lighting and special photo filter. Example photos of basalt are shown in Fig. 5. Subsequently, with the use of 'Fiji Is Just' open source digital image analysis software [5], image analysis was carried out to determine selected shape indicators.

Two shape factors [22] were chosen to determine:

- ▶ Aspect ratio (AR):

$$AR = \frac{L}{W} \quad (2)$$

The aspect ratio of a particle describes its form using a 2-dimensional system. It is defined as the ratio of the particle's length (L) to width (W) (Fig. 6). The aspect ratio of circle and equilateral polygon is 1.

► Roundness (R):

The value of roundness is equal to or greater than 1. The roundness describes how close a particle shape is to a circle.

$$R = \frac{l^2}{4\pi A} \quad (3)$$

where:

l – perimeter in 2-dimensional projection,

A – area in 2-dimensional projection (Fig. 6).

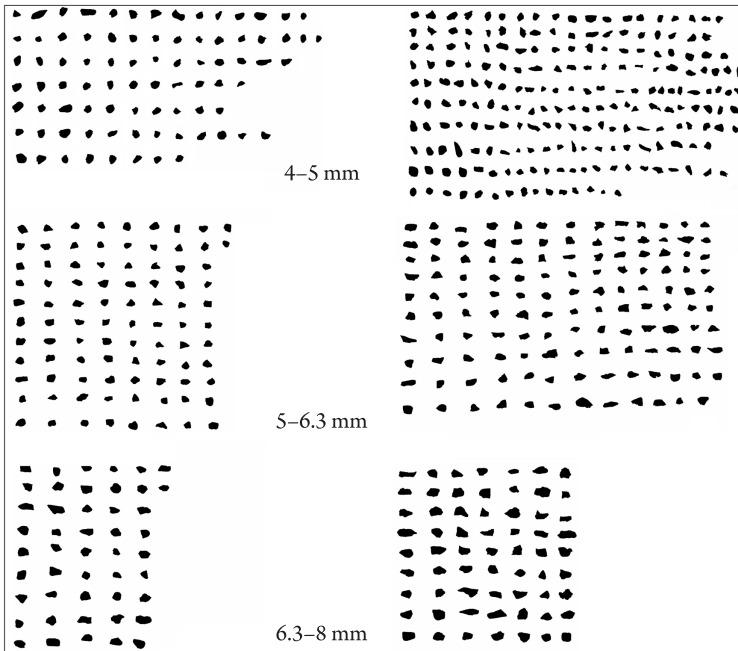


Fig. 5. Top view of regular (on left side) and irregular (on right side) basalt coarse particles

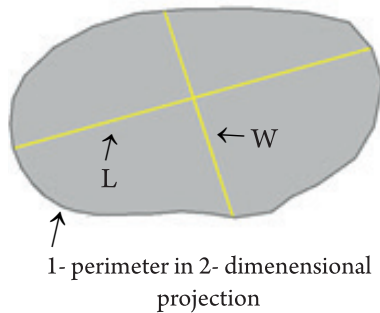


Fig. 6. An aggregate image with the length, width and perimeter in a 2-dimensional projection

Aspect ratio and roundness are based on 2-dimensional analysis. In order to obtain more accurate results, regular and irregular coarse aggregate should be compared with each other using 3-dimensional shape indicators [22].

## 5. Results and discussion

For regular and irregular coarse aggregate, statistical parameters were determined, such as: mean values, standard deviations and coefficients of variation of the two shape factors (aspect ratio and roundness). Statistical data was calculated for both the entire range of particle sizes 4–8 mm and the different grades: 4–5 mm, 5–6.3 mm and 6.3–8 mm. Complete statistical parameters for regular coarse aggregates of basalt and porphyry are presented in Table 1; these values for the irregular coarse aggregates of basalt and porphyry are presented in Table 2. In addition, Table 3 shows the results for regular and irregular granite coarse aggregate in 4–8 mm size fraction [17].

Table 1. Statistical parameters for shape factors of regular basalt and porphyry coarse aggregate

Regular basalt coarse aggregate							
Shape parameters	Size fractions [mm]	Valid N	Mean	Minimum	Maximum	Std. dev.	Coef. var. [%]
AR	4–5	83	1.424	1.048	3.051	0.369	25.883
	5–6.3	90	1.378	1.039	2.438	0.244	17.740
	6.3–8	47	1.484	1.055	2.389	0.323	21.739
	4–8	220	1.418	1.039	3.051	0.314	22.147
R	4–5	83	1.524	1.272	2.114	0.160	10.513
	5–6.3	90	1.365	1.195	1.812	0.110	8.026
	6.3–8	47	1.378	1.167	1.689	0.118	8.568
	4–8	220	1.428	1.167	2.114	0.152	10.631
Regular porphyry coarse aggregate							
Shape parameters	Size fractions [mm]	Valid N	Mean	Minimum	Maximum	Std. dev.	Coef. var. [%]
AR	4–5	106	1.518	1.027	3.154	0.404	26.645
	5–6.3	115	1.414	1.018	2.930	0.301	21.273
	6.3–8	50	1.373	1.015	2.196	0.253	18.415
	4–8	271	1.447	1.015	3.154	0.342	23.624
R	4–5	106	1.408	1.176	2.169	0.169	12.032
	5–6.3	115	1.463	1.258	2.075	0.157	10.751
	6.3–8	50	1.423	1.239	1.709	0.119	8.353
	4–8	271	1.434	1.176	2.169	0.158	10.983

Table 2. Statistical parameters for shape factors of irregular basalt and porphyry coarse aggregate

<b>Irregular basalt coarse aggregate</b>							
<b>Shape parameters</b>	<b>Size fractions [mm]</b>	<b>Valid N</b>	<b>Mean</b>	<b>Minimum</b>	<b>Maximum</b>	<b>Std. dev.</b>	<b>Coef. var. [%]</b>
<b>AR</b>	4-5	207	1.575	1.055	3.875	0.474	30.090
	5-6.3	129	1.630	1.029	3.034	0.462	28.352
	6.3-8	63	1.653	1.025	3.371	0.486	29.394
	4-8	399	1.605	1.025	3.875	0.472	29.405
<b>R</b>	4-5	207	1.552	1.203	2.703	0.246	15.833
	5-6.3	129	1.491	1.232	2.160	0.187	12.519
	6.3-8	63	1.472	1.229	2.151	0.198	13.428
	4-8	399	1.519	1.203	2.703	0.223	14.675
<b>Irregular porphyry coarse aggregate</b>							
<b>Shape parameters</b>	<b>Size fractions [mm]</b>	<b>Valid N</b>	<b>Mean</b>	<b>Minimum</b>	<b>Maximum</b>	<b>Std. dev.</b>	<b>Coef. var. [%]</b>
<b>AR</b>	4-5	253	1.568	1.029	4.761	0.475	30.271
	5-6.3	160	1.552	1.018	3.552	0.441	28.423
	6.3-8	63	1.560	1.037	3.235	0.455	29.143
	4-8	476	1.561	1.018	4.761	0.460	29.464
<b>R</b>	4-5	253	1.460	1.136	2.703	0.198	13.536
	5-6.3	160	1.526	1.211	2.915	0.250	16.353
	6.3-8	63	1.468	1.247	2.110	0.175	11.897
	4-8	476	1.483	1.136	2.915	0.216	14.534

Table 3. Statistical parameters for shape factors of regular and irregular granite coarse aggregate

<b>Regular coarse aggregate</b>						
<b>Shape parameters</b>	<b>Size fraction [mm]</b>	<b>Mean</b>	<b>Minimum</b>	<b>Maximum</b>	<b>Std. dev.</b>	<b>Coef. var. [%]</b>
<b>AR</b>	4-8	1.496	1.032	3.093	0.339	22.693
<b>R</b>	4-8	1.371	1.181	1.859	0.113	8.236
<b>Irregular coarse aggregate</b>						
<b>Shape parameters</b>	<b>Size fraction [mm]</b>	<b>Mean</b>	<b>Minimum</b>	<b>Maximum</b>	<b>Std. dev.</b>	<b>Coef. var. [%]</b>
<b>AR</b>	4-8	1.645	1.032	3.473	0.429	26.076
<b>R</b>	4-8	1.427	1.172	2.075	0.163	11.390

For both shape parameters, a value of 1 indicates that the shape is completely circular. It has been proven that the shape of regular coarse aggregate is closer to the shape of a circle than shapes of irregular coarse aggregate. It is worth noting that the selected shape factors are based on 2-dimensional analyses. Therefore, in subsequent tests, 3-dimensional analysis will be performed.

Analysing particle grade 4-8 mm of coarse aggregate, it can be said that:

- ▶ The AR shape factor for regular grains has the lowest value for basalt coarse aggregate and the highest for granite. For the irregular aggregate, the highest value of AR is for granite and the lowest for porphyry.
- ▶ The R shape factor for regular grains has the lowest value for granite coarse aggregate and the highest for porphyry. For the irregular aggregate, the highest value of R is for basalt and the lowest for granite.

Pearson's Chi-squared test has been used to verify the normality and log-normality distribution of the selected shape factors. Three hypothesis were assumed:

- ▶  $H_0$  states that the distribution is a normal distribution.
- ▶  $H_1$  states that the distribution is a log-normal distribution.
- ▶  $H_2$  states that the distribution is a generalised extreme value distribution.

Histograms and the Chi-square test results [12, 13] are presented in Figs. 7a, 7b and Figs. 8a, 8b. The confidence level was set at 95%. On analysis of the results, it can be observed that the assumption of normal or log-normal distribution was not fulfilled in any case. The assumption of generalised extreme value distribution was fulfilled for both shape factors in every case.

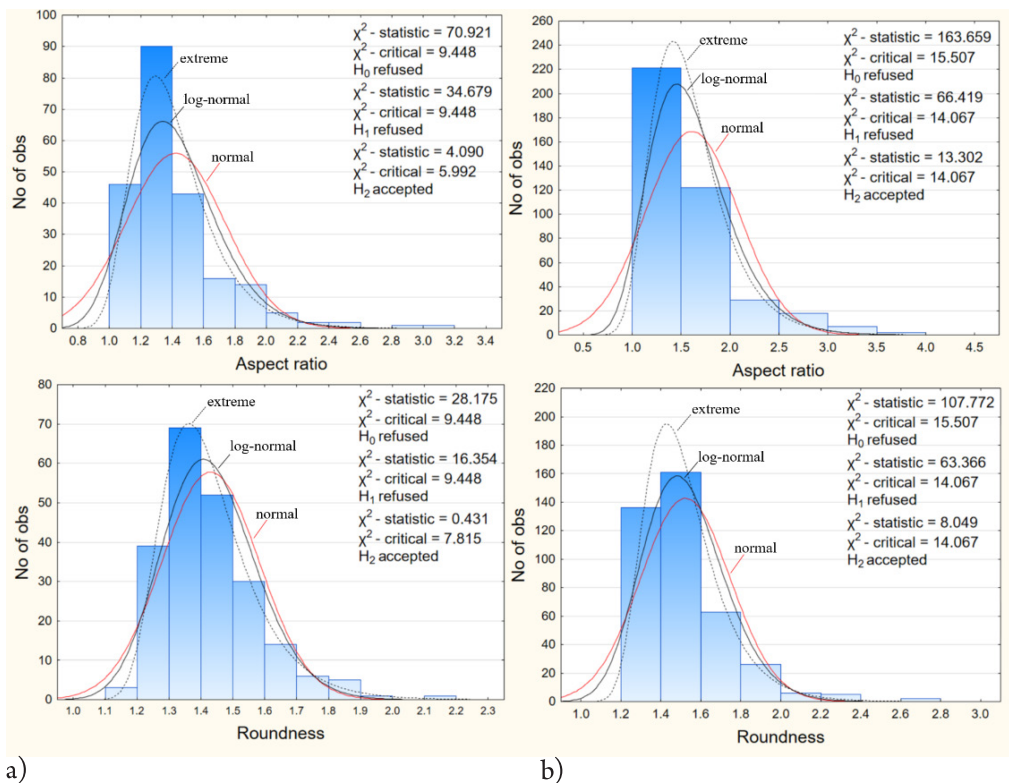


Fig. 7. Histograms and Chi-square test results for the normal, log-normal distribution and generalised extreme value distribution of AR and R of: a) regular basalt coarse particles; b) irregular basalt coarse particles

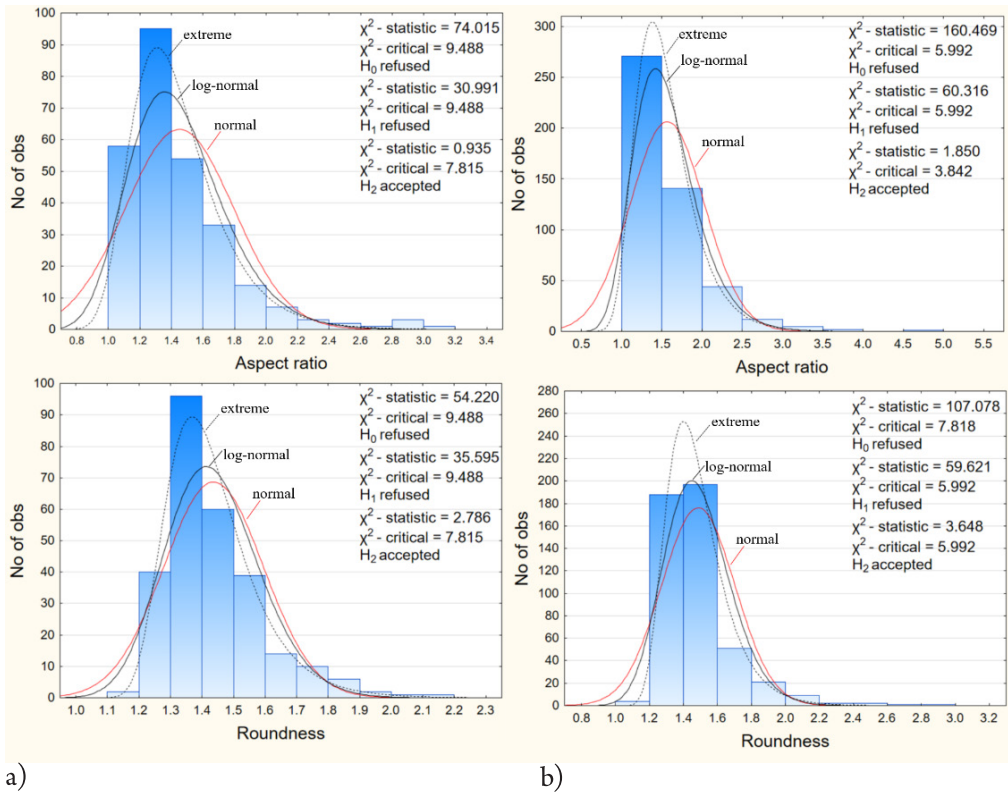


Fig. 8. Histograms and Chi-square test results for the normal, log-normal and generalised extreme value distribution of AR and R of: a) regular porphyry coarse particles; b) irregular basalt coarse particles

## 6. Conclusions

This work presents an experimental investigation of the comparative analysis of the coarse aggregate shapes used to manufacturing high-performance, self-compacting concrete. The main conclusions of the tests are as follows:

1. The FI indicator allows the quantitative assessment of regular and irregular coarse aggregate shapes. With the same crushing technology, the highest percentage of regular coarse aggregate was achieved for granite and the lowest for basalt.
2. The aspect ratio and roundness allows the qualitative assessment of regular and irregular coarse aggregate shapes. The following dependences have been shown:
  - ▶ according to AR shape factor, the regular coarse aggregate of basalt has the best quality;
  - ▶ the irregular coarse aggregate of porphyry has the lowest AR shape factor value;
  - ▶ according to R shape factor, the regular coarse aggregate of granite has the best quality;
  - ▶ the irregular coarse aggregate of granite has the lowest value for the R shape factor.
3. The best fitting distribution for aspect ratio and roundness at a 95% confidence level is the generalised extreme value distribution.

## References

- [1] Al-Rousan T., Masad E., Tutumluer E., Pan T., *Evaluation of image analysis techniques for quantifying aggregate shape characteristics*. Construction and Building Materials, 2007, 978–990.
- [2] Bangaru R.S., Das A., *Aggregate shape characterization in frequency domain*. Construction and Building Materials, 2012, 554–560.
- [3] Gawenda T., *Układ urządzeń do produkcji kruszyw foremnych*, AGH w Krakowie, Zgłoszenie nr P. 408045 z dn. 2014-04-28, Biuletyn Urzędu Patentowego, 2015 nr 23.
- [4] Krishnamurthy Pandurangan, Kothandaraman S., *Effect of Coarse Aggregate Size And Shape on the Strength and Flow Characteristics of Self-compacting Concrete*. ICI Journal, 2012.
- [5] <http://fiji.sc> [access: 10.06.2018].
- [6] Junaid Mansoor, Syed Adnan Raheel Shah, Mudasser Muneer Khan, Abdullah Naveed Sadiq, Muhammad Kashif Anwar, Muhammad Usman Siddiq, Hassam Ahmad, *Analysis of Mechanical Properties of Self Compacted Concrete by Partial Replacement of Cement with Industrial Wastes under Elevated Temperature*. Applied Sciences, 2018, 8, 364.
- [7] Karamloo M., Mazloom M., Payganeh G., *Effects of maximum aggregate size on fracture behaviors of self-compacting lightweight concrete*, Construction and Building Materials, 2016, 508–515.
- [8] Kostrzanowska-Siedlarz A., Gołaszewski J., *Rheological properties of High Performance Self-Compacting Concrete: Effects of composition and time*. Construction and Building Materials, 2016, 705–715.
- [9] Koziół W., Ciepliński A., Machniak Ł., Borcz A., *Kruszywa w budownictwie. Cz. 1. Kruszywa naturalne*, Nowoczesne Budownictwo Inżynieryjne, 2015, 98–100.
- [10] Kuo C.Y., Freeman R., *Imaging indices for quantification of shape, angularity, and surface texture of aggregates*, Transportation Research Record, 2000, 57–65.
- [11] Małolepszy J., Deja J., Brylicki W., Gawlicki M., *Technologia betonu – metody badań*, Uczelniane Wydawnictwa Naukowo-Dydaktyczne AGH, Kraków 2000.
- [12] McHugh M.L., *The Chi-square test of independence*, Biochemia Medica, 2013, 23 (2), 143–149.
- [13] Miller R., Siegmund D., *Maximally selected Chi-square statistics*, Biometrics, 1982, 38, 1011–1016.
- [14] Navarrete I., Lopez M., *Understanding the relationship between the segregation of concrete and coarse aggregate density and size*, Construction and Building Materials, 2017, 741–748.
- [15] Okamura H., Ouchi M., *Self-compacting concrete*, Advanced Concrete Technology, 2003, 5–15.
- [16] Ostrowski K., *The influence of coarse aggregate shape on the properties of high-performance, self-compacting concrete*, Technical Transaction, 2-B/2017, 25–33.
- [17] Ostrowski K., Sadowski Ł., Stefaniuk D., Wałach D., Gawenda T., Oleksik K., Usyduś I., *The effect of the shape of the coarse aggregate on the properties of self-compacting high-performance fibre-reinforced concrete*, Materials – in press.

- [18] Ostrowski K., Sadowski Ł., Wałach D., Gawenda T., *The influence of coarse aggregate shape on the properties of self-compacting high-performance fibre-reinforced concrete*, RILEM Publications S.A.R.L., 2017.
- [19] PN-EN 933-4:2008 Badania geometrycznych właściwości kruszyw. Część 4: Oznaczenie kształtu ziarn. Wskaźnik kształtu, 2008.
- [20] Rajan B., Singh D., *Understanding influence of crushers on shape characteristics of fine aggregates based on digital image and conventional techniques*, Construction and Building Materials, 2017, 833–843.
- [21] Smarzewski P., Barnat-Hunek D., Jezierski W., *The possibility of using boiler slag as coarse aggregate in high strength concrete*. KSCE Journal of Civil Engineering, 2017, 22, 1816–1826.
- [22] Xianglin Gu, Yvonne Tran, Li Hong, *Quantification of coarse aggregate shape in concrete*, Front. Struct. Civ. Eng, 2014, 8, 308–321.
- [23] Xiaoxin Zhang, Gonzalo Ruiz, Manuel Tarifa, David Cendón Francisco Gálvez, Waleed H. Alhazmi, *Dynamic Fracture Behavior of Steel Fiber Reinforced Self Compacting Concretes (SFRSCCs)*, Materials, 2017, 10: 1270.